

Electrodeposition of Cu-Sn and Ag-Sn alloys from thiourea containing electrolytes

M. Bestetti, A. Vincenzo and P.L. Cavallotti

Dip. Chimica, Materiali e Ingegneria Chimica, Politecnico di Milano, Milano, Italy

The electrodeposition of copper-tin and silver-tin alloys from non-cyanide electrolytes has been recently the subject of intensive research. These alloys are suitable materials for several applications, both for engineering and decorative purposes; in particular, they are of special interest for lead-tin solderable finishes replacement. The large difference between the standard potential of Cu(II) or Ag(I) and Sn(II) requires the use of strong complexing agents. Thiourea, (CS(NH₂)₂), is a strong ligand for both Cu(I) and Ag(I) in acidic solution. In the present work, chemically stable and operatively reliable plating baths for the electrodeposition of Cu-Sn and Ag-Sn alloys, in the entire composition range and up to 25%Sn respectively, are presented. The relationship between the structure of the electrodeposited phases and the main operating conditions is investigated. Phase diagrams for ECD alloys are proposed and compared to equilibrium phase diagrams. Electrodeposited copper-tin alloys from simple acidic solutions are characterized by the following sequence of structures: fcc, hcp, cubic, pseudo-hexagonal and tetragonal β -Sn, at increasing tin content into the deposits. A characteristic of thiourea containing baths is the electrodeposition of an amorphous phase, when sulfur is incorporated into the deposits and Sn content is in the range 15% to 40%. Electrodeposited silver-tin alloys are obtained with fcc, hcp or biphasic hcp+ β Sn crystal structure, with exclusion of the ordered intermetallic phase. Mechanical properties and thermal stability of ECD alloys are also discussed in relation to their phase structure.

For more information, contact:

P. L. Cavallotti

Dip. Chimica, Materiali, Ingegneria Chimica "Giulio Natta" – Politecnico di Milano

Via Mancinelli,7 - 20131 Milano, Italy

Phone: +39-02-23993149

Fax: +39-02-23993180

E-mail: pietro.cavallotti@polimi.it

Introduction

Copper-tin and silver-tin alloys electrodeposition is an important research topic for electroplaters, since these alloy coatings have a wide range of applications. However, their electrodeposition process presents critical issues related to solutions chemistry, process reliability and plating bath maintenance.

Bronze deposits are among the most important electrodeposited alloys. Yellow and white bronzes are mainly used for decorative and protective purposes, in particular as a substitute for nickel, and could be a valuable choice as engineering coatings in many application, due to high hardness and wear resistance, protection against corrosion (white bronzes) and good solderability¹. New application possibilities are envisaged in microelectronics for alloys with low Sn or Cu content. Cu(Sn) alloys are interesting as interconnection material for integrated circuits, as they show higher electromigration resistance compared to copper interconnects². Sn(Cu) alloy plating is being evaluated as a possible whisker free alternative to Sn(Pb) solderable coatings³.

Commercial solutions for Cu-Sn alloy plating are alkaline electrolytes containing copper–cyanide complexes and stannate. Cyanide free bath, either alkaline or acidic, have been proposed but none of them has achieved practical importance⁴.

Ag-Sn electrodeposition, apart from Sn(Ag) solder alloy, was also reported from alkaline baths, such as silver cyanide - tin pyrophosphate⁵⁻⁷ or silver iodide - tin pyrophosphate baths⁸. Electrodeposited Ag-Sn alloys are attractive for both decorative finishing and engineering applications, since they provide improved tarnish resistance and superior mechanical properties to silver or copper substrates⁹. Interesting application could be for finishing of low voltage contacts¹⁰ and as anti-tarnish protection of silverware, maintaining good aesthetic appearance more easily than silver.

In this work, cyanide free baths for Cu-Sn and Ag-Sn alloy plating with acidic thiourea solutions is proposed. The electrodeposition of a wide composition range of alloys, as well as of the single metal Ag and Cu, was successfully achieved from

acidic solutions based on Ag(I) or Cu(I) – thiourea complexes¹¹.

Experimental

Plating solutions were prepared from analytically pure chemical reagents and double distilled water.

The composition of the Ag-Sn plating solution is reported in Table 1. Electrodeposition is carried out at room temperature in stagnant solution on polished brass sheets, coated with a thin silver displacement film. The displacement bath is a simple acidic solution of composition CS(NH₂)₂ 1M, H₂SO₄ 0.5M Ag(I) 0.05M and KBr 500ppm.

The electrolyte composition for Cu-Sn alloys electrodeposition is similar to that of Ag-Sn bath (see Table 2). On the other hand, operation conditions are very different, depending upon the Cu(I)/Sn(II) and Tu/Cu(I) ratios in solution. Temperature is in the range from 30°C to 60°C and intensive stirring of the electrolyte is required.

Table 1
Composition of Ag-Sn Alloys Plating Solutions

Chemicals	Concentration M
Ag ₂ CO ₃	0.025÷0.1
CS(NH ₂) ₂	1÷2
SnSO ₄	0.025÷0.075
H ₂ SO ₄	0.5÷1
Pyrocathecol	0.025÷0.05
KI	0.5÷1·10 ⁻³

Table 2
Composition of Cu-Sn Alloys Plating Solutions

Chemicals	Concentration M
Cu ₂ O	0.01÷0.2
CS(NH ₂) ₂	0.2÷1.5
SnSO ₄	up to 0.1
H ₂ SO ₄	1
Pyrocathecol	up to 0.1

Polished steel or brass sheets were used as substrate; before plating, they were slightly etched respectively in dilute hydrochloric or sulfamic acid, thoroughly rinsed in distilled water and dried with nitrogen.

Deposits phase structure was determined by X-ray diffractometry (XRD) with $\text{CuK}\alpha$ radiation and a powder goniometer. Surface morphology was investigated by Scanning Electron Microscopy (SEM). Deposits composition was determined by Energy Dispersion Spectroscopy (EDS).

Vickers microhardness (HV) and elastic modulus (E) data were obtained from penetration depth-load curves by means of FISCHERSCOPE[®] H100 Microhardness Measurement System. Measurements were carried out on the samples surface with peak load from 100 to 1000mN, also assessing the effect of the applied load on HV and E values. The difference between HV and E data obtained at minimum and maximum load in the examined range was within the standard deviation of the observed values. Cross section measurements were performed in some cases, showing good agreement with surface microindentation results.

Results and discussion

Silver-Tin Electrodeposition

The simple acidic silver - thiourea solution is not suitable for plating, because of the onset of cathodic passivation at potential about -0.45V vs Ag/AgCl . The discharge of $\text{Ag}(\text{Tu})_3^+$ (overall stability constant, $\log K$ 13.4)¹² takes place at potential slightly less than -0.4V , as shown by the black line in Fig. 1, with low overvoltage. In galvanostatic condition, the maximum attainable cd is about $1\text{mA}/\text{cm}^2$. At a potential of about -0.45V a new cathodic process starts, giving a cd increase, followed by brightening and bluing of the electrode surface, as a consequence of sulfur incorporation into the deposit (up to 5%at according to EDS analysis). This behavior may be related either to chemisorption of thiourea oxidation products¹³ or to electroreduction of formamidine disulfide with formation of poisoning intermediates or reaction products containing sulfide¹⁴; no direct evidence we have so far about the mechanism of the observed surface blocking effect. The addition of KI 100ppm reactivates the surface, enabling a fivefold increase of the deposition cd (blue line in Fig. 1). In the presence of SnSO_4 0.025M, Ag-Sn alloys coatings can be electrodeposited in a relatively small potential range, at cd $4\text{--}8\text{mA}/\text{cm}^2$ (red line in Fig.

1). Hydrogen evolution becomes possible at potential below -0.65V .

The composition of ECD Ag-Sn alloys is determined both by deposition cd and by Sn^{2+} concentration (see Fig. 2). Sn content in the alloy varies in a relatively small range with increasing deposition cd , at fixed $[\text{Sn}^{2+}]$ in the bath, while, at fixed cd , a wider range of composition can be obtained changing $[\text{Sn}^{2+}]$.

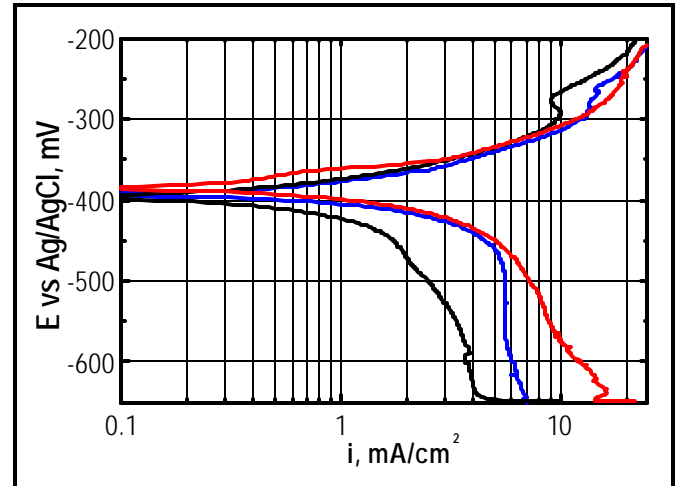


Fig. 1 – Low scan polarization curves at $\text{Ag}99.9\%$ electrode in the following solutions: H_2SO_4 0.75M, Tu 2M, $\text{Ag}(I)$ 0.1M (black line); same with addition of KI 100ppm (blue line); plus SnSO_4 0.025M (red line). Room temperature, stagnant electrolyte, $0.2\text{mV}/\text{s}$.

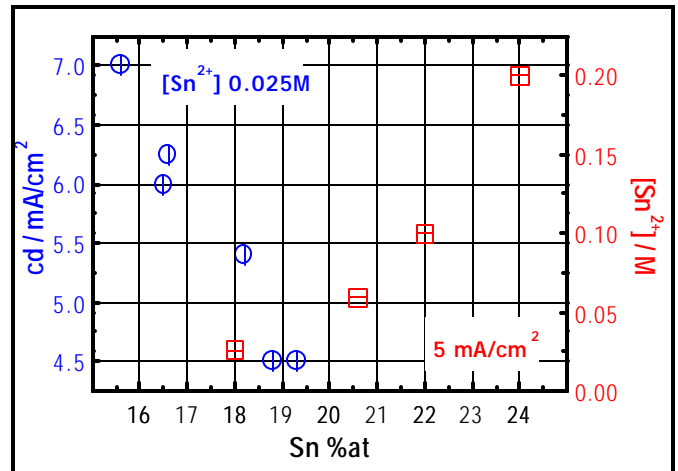


Fig. 2 – Relationship between $\text{Sn}\%at$ in ECD Ag-Sn alloys and deposition cd , at $[\text{Sn}^{2+}]$ 0.025M, and $[\text{Sn}^{2+}]$ in the bath, at cd $5\text{mA}/\text{cm}^2$; room temperature, stagnant solution, $5\mu\text{m}$ thick coatings on silver-coated brass.

ECD Ag-Sn alloys, in the composition range 13÷24at.%Sn, have an hexagonal close packed structure, similar to that of the metallurgical ζ phase. The intermetallic compound Ag_3Sn (ϵ -phase, with orthorhombic lattice) present in the phase diagram with a small composition range, is not obtained by electrodeposition. The axial ratio c/a of electrodeposited hcp alloys changes with the electronic concentration (number of valency electrons to number of atoms ratio, e/a) in agreement with the results reported by King and Massalski for metallurgical ζ phases¹⁵. The ECD ζ phase Ag_xSn shows either a low [10.1] or [00.1] preferred orientation (PO) (see Fig. 3), with bright and matte appearance respectively, depending on Sn content.

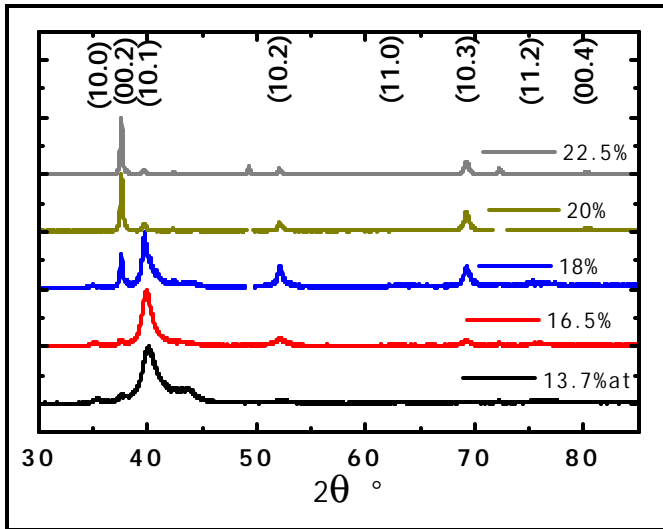


Fig. 3 – XRD patterns of Ag-Sn alloy coatings on brass, electrodeposited at room temperature and cd in the range 4÷10mA/cm² from base solution: H_2SO_4 0.75M, Tu 2M, Ag(I) 0.1M, KI 300ppm, changing Sn^{2+} concentration from 0.025M to 0.07M.

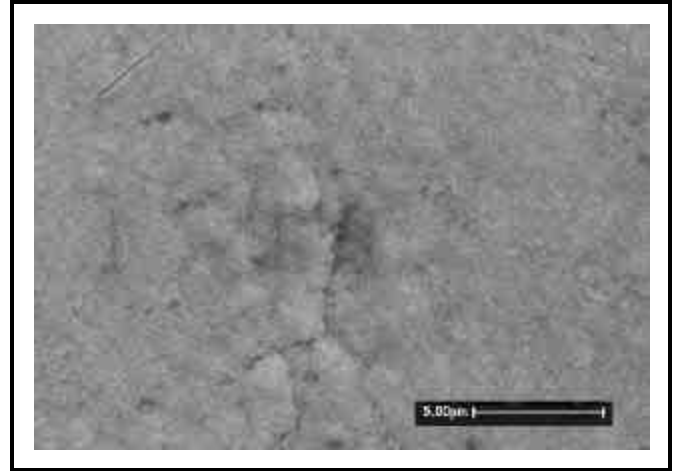


Fig. 4 – SEM surface micrograph of a Ag-Sn16.5%at alloy layer electrodeposited at room temperature and cd 6.5mA/cm², from H_2SO_4 0.75M, Tu 2M, Ag(I) 0.1M, KI 300ppm, SnSO_4 0.025M.

Appearance, PO and Sn content in the alloy depend on the deposit microstructure: when Sn% is <18%at, the (10.1) peak prevails in XRD patterns and crystal size, derived from the diffraction peak broadening and also from morphological examination (see Fig. 4), is below 10 nm; broadening and asymmetry of (10.1) diffraction peak increases at decreasing Sn%.

The crystal structures of alloys with Sn content outside the composition range corresponding to the hcp ζ phase, conform to the equilibrium phase diagram, but without the ϵ phase. For Sn content <11%at, deposits show the fcc structure of the α -Ag phase, not far from the maximum Sn solubility of 11.5%at in α -Ag at 724°C; when Sn content in the alloy is >24%at, deposits have a biphasic ζ + β Sn structure, and growth tends to become morphologically unstable, giving powdery deposits with time. Sn rich alloys were obtained from solution based on methanesulphonic acid with low Ag(I) concentration and ratio $[\text{Tu}]/[\text{Ag}^+]$ about 10; but these baths tend to become unstable with time and should be greatly improved to acquire technical relevance.

Fig. 5 show the composition range of the different phases observed in the electrodeposited Ag-Sn alloys from acidic thiourea solutions.

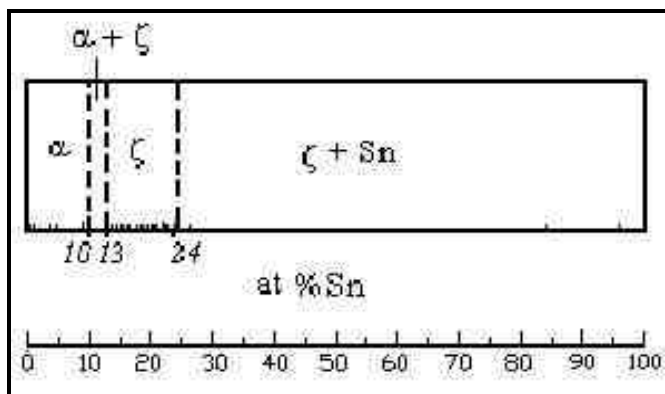


Fig. 5 – Phase structure of electrodeposited Ag-Sn alloys.

As already mentioned, the crystal structure of ECD alloys follows the equilibrium phase diagram, with some noteworthy differences: the extension of the ζ phase field, the phase boundary moving from the equilibrium value of 18%at, at about 200°C, to 24%at Sn content, and the concomitant suppression of the ordered intermetallic (ϵ phase).

This is confirmed by heat treating ECD alloys with composition corresponding to the $\zeta+\epsilon$ two-phase region in the phase diagram. After 2hr at 250°C, ECD Ag-Sn23.5%at powder samples clearly show the appearance of the equilibrium ϵ phase, with orthorhombic lattice, and the change of the ζ phase lattice parameters towards the values corresponding to the solubility limit. In fact, the axial ratio c/a changes from 1.603 to 1.618, that is, Sn content of the ζ phase changes from about 23.5%at to 18.5%at, in accordance with the equilibrium phase diagram. A similar effect is observed when heat-treating thin films; however, no formation of ordered intermetallic is observed, possibly because it grows in a finely divided form, which does not give rise to detectable X-ray reflections.

Ag-Sn(14÷22%at) films were tested as anti-tarnish finish on ECD silver, according to the ISO 4538:1998 standard, showing that the Ag-Sn top layer can be a valuable protection at thickness as low as 0.3 μ m.

Microhardness and elastic modulus data, derived from indentation curves on 5 μ m thick deposits having ζ phase structure, are reported in Fig. 6. In the composition range 12 to 22%at Sn, both microhardness and elastic modulus show minor

changes. Cross-section measurements on thick coatings (30 μ m, 20÷22at%Sn), at 0.5N peak load, gave 265HV microhardness and 85GPa elastic modulus.

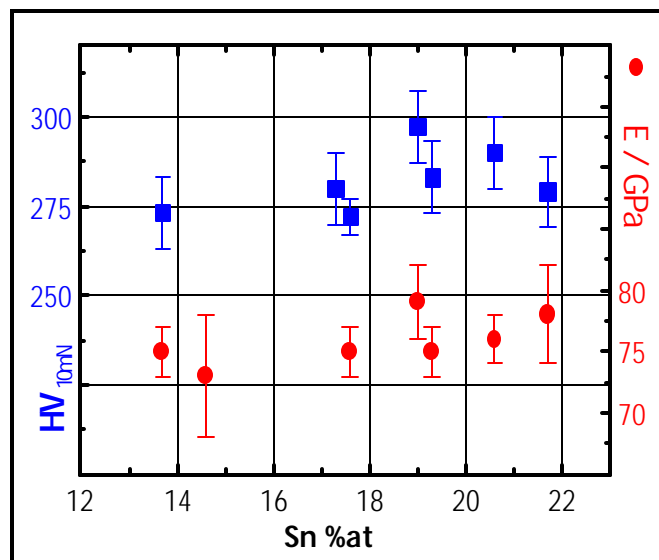


Fig. 6 – HV microhardness and elastic modulus of ECD Ag-Sn deposits versus Sn%at in the alloy. Data obtained by indentation depth – load measurements with peak load of 10mN on the surface of 5 μ m thick coatings deposited on brass substrate.

Copper-Tin Electrodeposition

The phase structure of electrodeposited Cu-Sn alloys was studied by Raub¹⁶ and Fedot'ev¹⁷ (cyanide solutions) and by Gorbunova¹⁸ and Watanabe¹⁹ (acid electrolytes). The investigators agree upon the formation of a supersaturated α -Cu(Sn) solid solution (up to 15% Sn content) and of the η phase (speculum, containing about Sn 45%), whilst there is no agreement upon the phase structure of alloys in the intermediate composition range. Besides, there is no report about the obtainment of the ordered ϵ phase with composition Cu₃Sn.

We studied the electrodeposition of copper-tin alloys from acid solutions, containing either cupric or cuprous salts. In this paper, results related to cuprous electrolytes are mainly presented and discussed.

Copper as Cu(I) was stabilized in acidic solution by thiourea addition which acts as a strong complexing agent for Cu(I) (logK 11.1 for Cu(CS(NH₂)₂)⁺ and logK 18.5 for Cu₂(CS(NH₂)₂)₂²⁺

at 20°C).²⁰ In this way it is possible to reduce the gap between copper and tin discharge potential as much as thiourea is added to the electrolyte. This is shown in Fig. 7, where potentiodynamic curves for a simple acidic Cu(II) sulfate solution and a thiourea–Cu(I) solution are compared.

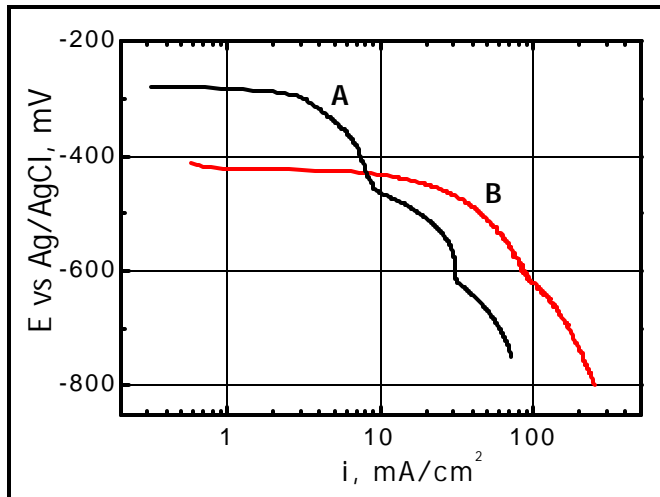


Fig. 7 – Polarization curves at Cu 99.99% electrode (1 mV/s) at 30°C (curve A) and 60°C (curve B) in stirred solutions; see text for electrolyte composition.

Curve A refers to CuSO₄ 0.1M, SnSO₄ 0.2M and H₂SO₄ 1M solution; curve B to Cu(I) 0.2M, Sn(II) 0.1M, CS(NH₂)₂ 0.8M, pyrocatechol 0.2M and H₂SO₄ 1M solution. Alloy deposition from the simple solution (A) is always preceded by deposition of Cu or α -Cu alloy; on the contrary, the potentiodynamic trace for solution B shows a single cd range, extending over two decades, where the alloy can be deposited. The slope change at -0.6V in both curves is related to the onset of hydrogen evolution.

The optimum deposition temperature is around 60°C. At lower temperature precipitation of copper thiourea sulfate compounds occurs, whilst higher temperature triggers thiourea oxidation.

The composition of alloy deposits depend on the molar ratios $[\text{CS}(\text{NH}_2)_2]/[\text{Cu}^+]$ and $[\text{Cu}^+]/[\text{Sn}^{2+}]$. For $[\text{CS}(\text{NH}_2)_2]/[\text{Cu}^+]$ 3 and $[\text{Cu}^+]/[\text{Sn}^{2+}]$ 4 to 10, Sn content is in the range 22 to 25at% at cd 2 to 10 mA/cm². In this composition range deposits with either crystalline (see Fig. 8) or near amorphous structure (see Fig. 9) are obtained. The structure type is likely related to the incorporation of sulfur during

growth. Amorphous like deposits can be obtained with Sn content in the range about 8 to 25%at and sulfur content up to 10%at (commonly 2 to 5%at). Sn and S content in the alloy coatings appear mutually related, as shown in Fig. 10; with Sn content above about 7-8at%, sulfur is incorporated into the deposits and its content increases with Sn%, reaching a maximum of about 10%at around Sn 20%at; with further increase of Sn%, sulfur content decreases.

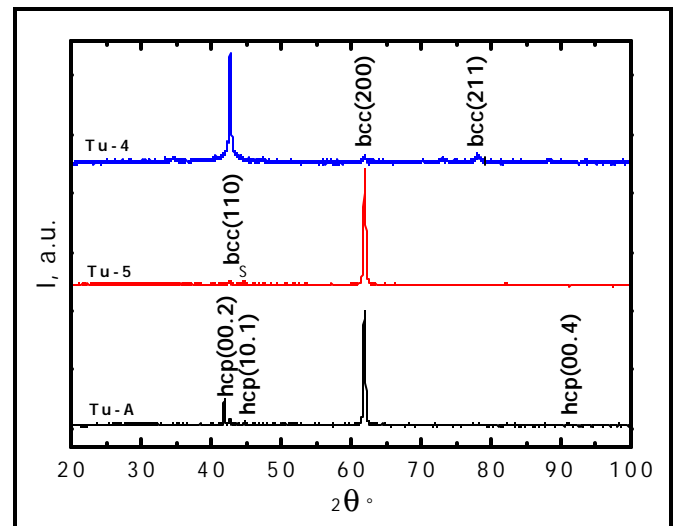


Fig. 8 - XRD patterns of Cu-Sn alloys coatings: Tu-4 Sn 25%at, S ~0.8%at; Tu-5 Sn 22%at, S below EDS detection limit; Tu-A Sn 22%at, S ~1%at. Electrolyte composition: Cu(I) 0.2M, CS(NH₂)₂ 0.6M, Sn(II) 0.05M, H₂SO₄ 1M; 60°C, 10mA/cm².

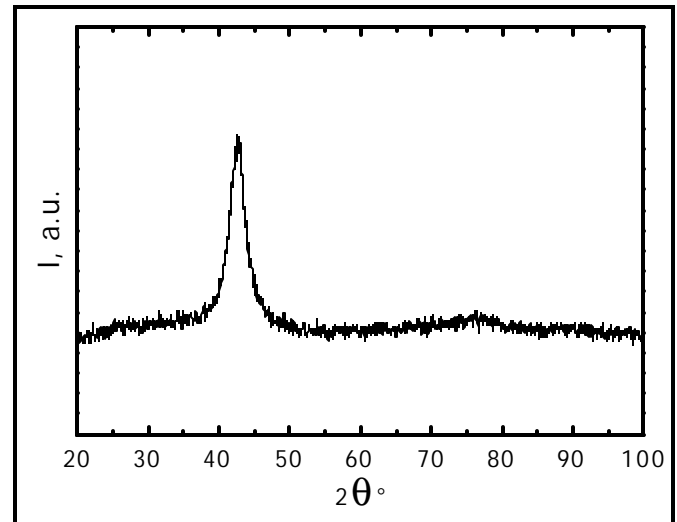


Fig. 9 - XRD patterns of amorphous ECD Cu-Sn alloys: Tu-3 Sn 23at%, S 3.5%; electrolyte composition: Cu(I) 0.2M, CS(NH₂)₂ 0.6M, Sn(II) 0.02M, H₂SO₄ 1M; 60°C, 10mA/cm².

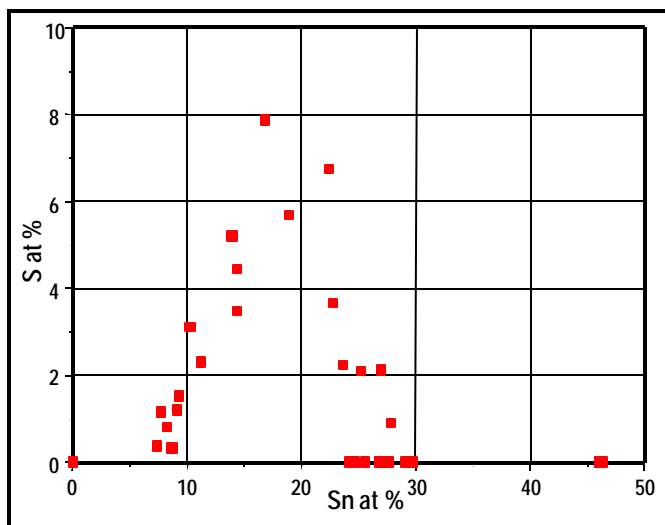


Fig. 10 – Sulfur content in ECD Cu-Sn alloys deposited from thiourea electrolytes.

The possible incorporation of sulfur is only slightly influenced by electrodeposition conditions, such as cd and thiourea concentration. As a rule, when Sn content is in the range about 8 to 20%at, alloy coatings contain sulfur and show the amorphous like structure. For Sn% above 20%at, sulfur can be incorporated in the coatings and deposits show the amorphous like structure for S%at above about 2-2.5%at. The observed structures can be related to fcc or hcp crystal lattice, when Sn content is below about 15%at, and to bcc crystal lattice for Sn% above 20%at (following the structure indexing proposed for crystalline deposits with similar composition). Thus, Sn content in the alloy or, in other words, tin concentration in the electrolyte, given the relative electrochemical nobility between Cu and Sn, appears as an important factor influencing sulfur incorporation in the coatings.

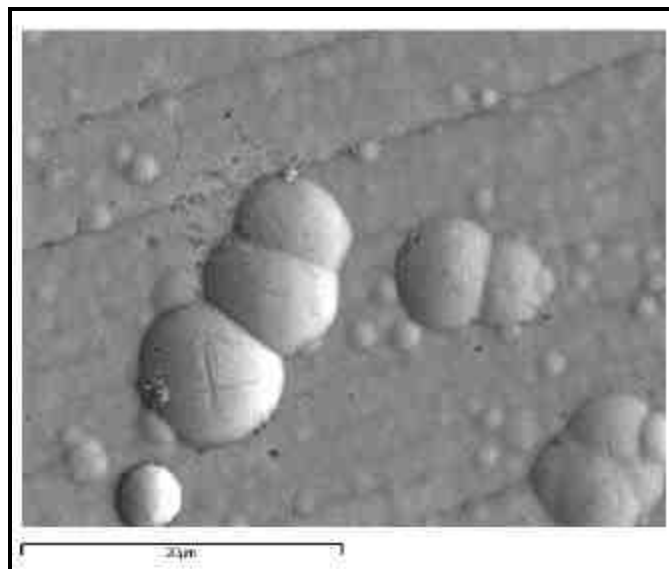


Fig. 11 – Surface morphology of a copper tin layer (Cu 91 at%, Sn 8.7at%, S 0.3at%). Cu(I) 0.2M, CS(NH₂)₂ 0.6M, Sn(II) 0.02M, pyrocatechol 0.04M, H₂SO₄ 1M; 60°C, 10mA/cm².

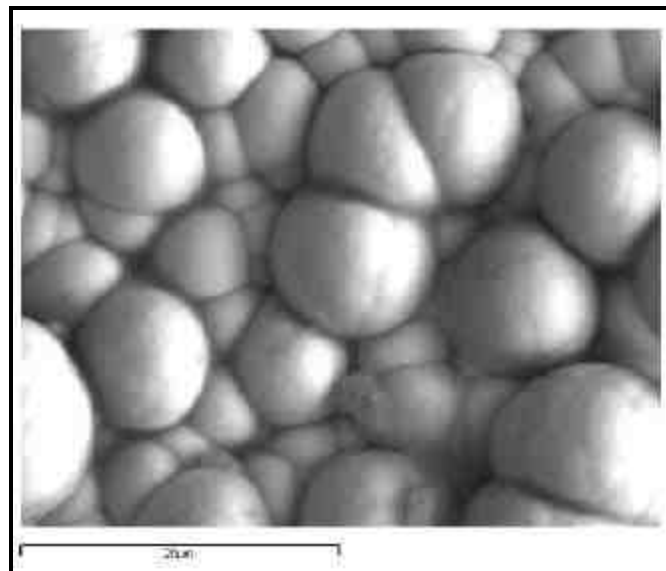


Fig. 12 – Surface morphology of copper tin layer (Cu 75.3 at%, Sn 16.9at%, S 7.8at%). Electrolyte composition: Cu(I) 0.2 M, CS(NH₂)₂ 0.8 M, Sn(II) 0.008 M, pyrocatechol 0.016 M, H₂SO₄ 1 M; 10 mA/cm², 60°C, gentle stirring.

Deposits morphology is particularly influenced by sulfur incorporation and can be related to the structure type. Fig. 11 shows the surface morphology of a Cu-Sn8.7%at sample with S content about 0.3%at. A featureless surface results with globular morphology.

This morphology is likely related to sulfur incorporation. In fact, as shown in Fig. 12, the formation of large globular features evenly distributed over the surface is observed with higher S content.

Increasing thiourea concentration in the electrolyte and as a consequence tin content in the alloy, morphology changes drastically, see Fig. 13, resulting from layering and overlapping of large platelets; no evidence of sulfur embedding results and deposits show crystalline structure.

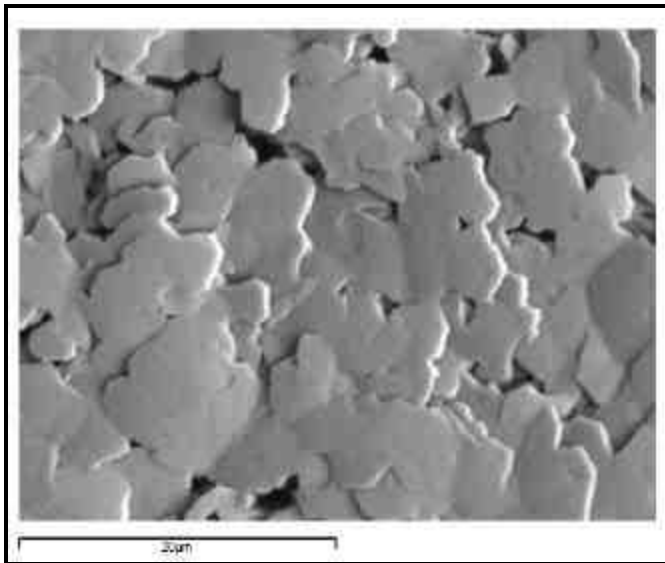


Fig. 13 – Surface morphology of Cu-Sn27at% alloy deposit from Cu(I) 0.2M, CS(NH₂)₂ 0.8M, Sn(II) 0.02M, pyrocathocol 0.04M, H₂SO₄ 1M, at 10 mA/cm², 60°C, under gentle stirring.

Further increase of thiourea concentration in the electrolyte allows the electrodeposition of Cu-Sn alloy coatings with phase structure corresponding to the η phase of the equilibrium diagram (Cu₆Sn₅). Fig. 14 shows XRD patterns of samples with Sn content in the range 45 to 47at%, electrodeposited from solution with [CS(NH₂)₂]/[Cu⁺] and [Cu⁺]/[Sn²⁺] ratios 4 to 5, at 20 mA/cm² and 60°C. Deposits show either [101] or [110] PO. The typical morphology of η-phase deposits, for Sn content about 45at%, is shown in Fig. 15: grains are in the shape of sharp-edged pyramids, with size increasing with deposition cd in the range 10 to 20mA/cm².

Increasing the [CS(NH₂)₂]/[Cu⁺] ratio or decreasing [Cu⁺]/[Sn²⁺] in the electrolyte, Sn content

in the coatings can be increased up to values around the eutectic composition. In this respect, a suitable electrolyte composition is the following: Cu(I) 0.01M, CS(NH₂)₂ 0.2M, Sn(II) 0.2M, pyrocathocol 0.2M, H₂SO₄ 1M. Sn(Cu) coatings with Sn% about 98%at can be obtained at 80mA/cm² and 45°C, with gentle stirring.

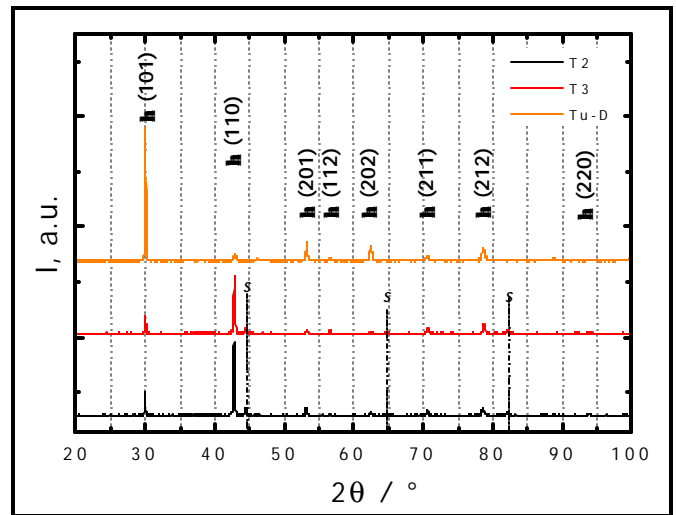


Fig. 14. XRD patterns of ECD Cu-Sn coatings with NiAs pseudo-hcp structure (T2 47at%; T3 45at%; Tu-D 46at%). Electrolyte composition: Cu(I) 0.3M, CS(NH₂)₂ 1.5M, Sn(II) 0.075M, pyrocathocol 0.15M (samples T2 and T3); Cu(I) 0.2M, CS(NH₂)₂ 1M, Sn(II) 0.05M, pyrocathocol 0.1M (sample Tu-D); H₂SO₄ 1M; 10 mA/cm², 60°C, gentle stirring.

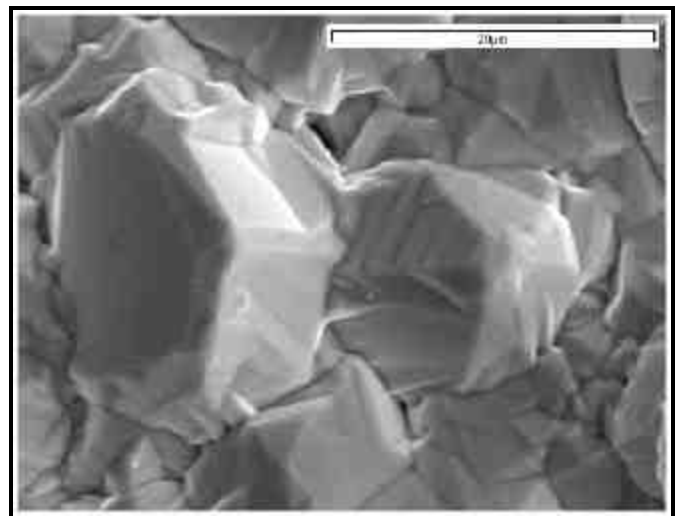


Fig. 15 – Surface morphology of Cu-Sn44%at deposit from Cu(I) 0.2M, CS(NH₂)₂ 1M, Sn(II) 0.05M, pyrocathocol 0.1M, H₂SO₄ 1M, at 20 mA/cm² and 60°C.

Mechanical properties of the alloy coatings are related to phase structure and, for bcc-indexed structure, also to amorphous or crystalline type, i.e. to sulfur content. Microhardness and elastic modulus of Cu-Sn coatings with Sn content in the range 20 to 23%at (bcc structure) are respectively about 500 HV and 150 GPa, at 250mN peak load (coatings with same composition from Cu(II) acidic solution show microhardness in the range 600 to 700 HV). Mechanical properties of these coatings are definitely impaired by sulfur incorporation into the deposits: microhardness can be decreased down to 200HV, elastic modulus down to 75GPa, with S content about 3.5%at. Coatings of the η -phase show microhardness in the range 470 to 500 HV and elastic modulus about 140 GPa (250mN peak load). These values are very close to those for alloy coatings with same composition and structure from Cu(II) acidic solution.

Conclusions

Ag-Sn alloys with Sn content up to 24%at (~26%wt) are obtained from acidic solutions containing $\text{CS}(\text{NH}_2)_2$ 2M, H_2SO_4 0.75M, $[\text{Ag}^+]$ 0.1M and SnSO_4 0.025÷0.07M, in the cd range 4÷10 mA/cm², at room temperature and without stirring.

As deposited layers are bright or semi-bright up to ~5 μm thickness, if Sn content is less than ~18%at.

In the composition range 13 to 25%at Sn content, alloys have the ζ phase crystal structure, with hcp lattice and axial ratio decreasing with increasing Sn content (as occurring in metallurgical alloys). No formation of ordered intermetallic compound (ϵ phase) is observed.

Ag-Sn alloys show tarnish resistance superior to Ag999 and ECD Ag. Microhardness is noticeably increased with respect to silver: 265±5 HV (500mN - 20s) compared with 100÷120 HV of ECD Ag films from acidic thiourea solution.

Electrodeposition of Cu-Sn alloys from acidic electrolytes is characterized by the following sequence of phases at increasing tin content: *fcc*, *hcp*, *bcc*, *NiAs type* (η), separated by biphasic fields.

The acidic electrolyte containing Cu(I)-thiourea complex and Sn(II) salts are stable and suitable for

electrodeposition of copper-tin alloys over the entire composition range. For instance, an electrolyte of composition Cu 0.2M, $\text{CS}(\text{NH}_2)_2$ 0.8M, Sn(II) 0.04M, H_2SO_4 1M, at 10 mA cm⁻² and 60°C, gives semi-bright bronze layers with tin content around 22-25 at% and cubic structure; another electrolyte of composition Cu 0.2M, $\text{CS}(\text{NH}_2)_2$ 1M, Sn(II) 0.05M, H_2SO_4 1M, at 10 mA cm⁻² and 60°C gives satin deposits, with Sn 43-47at% and NiAs-type structure.

The hcp phase was not observed until now in Co-Sn alloys electrodeposited from alkaline solutions, only an hexagonal superstructure as a ζ phase was reported by to be present between a cubic δ phase and the η phase by Fedotev et al¹⁷; whilst it was observed in layers codeposited with a secondary ion beam method²¹. From acidic solutions the presence of hcp phase is evident (and even the results of Arai and Watanabe⁸ can be reinterpreted in this perspective). An influence of the sulfur presence favoring this structure cannot be disregarded.

We have interpreted the cubic intermediate phase that we have observed, with composition about Cu_3Sn , as a bcc phase, but we cannot exclude a more complicated structure favored by short range order interaction, although this is not one of those reported for metallurgical alloys. Also in our case the metallurgical orthorombic ϵ phase, obtained in metallurgical alloys, is not observed.

In correspondence to the obtainment of the different phases the mechanical properties change, with relative maxima at composition near to stoichiometric values.

In conclusion, the structure of the observed Ag-Sn and Cu-Sn could be explained as the consequence of the great difficulty, almost impossibility, to obtain long range ordered structures by electrodeposition, whilst short range order influence is maintained. With this exclusion, it is possible to read the possible phases of electrodeposited alloys from free enthalpy/composition curves calculated according to this interpretation.

Acknowledgements

Thanks are due to D. Piconi (SEM-EDS), M. Ronchi (XRD), and F. Pagano (nanoindenter) for samples characterization.

References

- ¹ F. Simon, K. Leyendecker and F. Glaser, *Proc. AESF SUR/FIN® 2000*, 360 (2000).
- ² K.L. Lee, C.K. Hu, K.N. Tu, *J. Appl. Phys.* **78**, 4428 (1995).
- ³ M. Jordan, *Galvanotechnik* **92** 1225 (2001).
- ⁴ M. Jordan, *The Electrodeposition of Tin and its Alloys*, Eugen G. Leuze Publishers, Saulgau/Württ, D, 1993; p.155.
- ⁵ N. Kubota and E. Sato, *Electrochim. Acta*, **29** (1984) 361.
- ⁶ N. Kubota and E. Sato, *Electrochim. Acta*, **30** (1985) 305.
- ⁷ J. Cl. Puipe and W. Fluehmann, *Plat. & Sur. Finish.*, January '83 (1983) 46.
- ⁸ S. Arai and T. Watanabe, *Materials-Transactions-JIM.*, **39**(4), 439 (1998); *J. Japan Inst. Met.*, **60**(12) 1149 (1996).
- ⁹ A. Vicenzo, M. Bestetti, F. Pirovano and P.L. Cavallotti, *Abstract No. 661*, 200th ECS and 52th ISE Meeting; San Francisco (2001).
- ¹⁰ R. Nutsch, H. Liebscher, W. Degner, G. Hecht, *Galvanotechnik*, **84**, 425 (1993).
- ¹¹ P.L. Cavallotti, M. Bestetti, L. Magagnin, M. Seregini, A. Vicenzo; *Electrodeposition of copper and silver, and their alloys with tin from cyanide free electrolytes*; Italian Patent pending.
- ¹² I. V. Mironov, L. D. Tselodub, *Russ. J. Inor. Chem.*, **41**, 240 (1996).
- ¹³ M. Szklarczyk, N. Nhu Hoa, P. Zelenay, *J. Electroanal. Chem.*, **405**, 111 (1996).
- ¹⁴ A. Bolzàn, I.B. Wakenge, R.C. Salvarezza, A.J. Arvia, *J. Electroanal. Chem.* **475** (1999) 181.
- ¹⁵ H. W. King and T. B. Massalski, *Phil. Mag.*, **6**, 669 (1961).
- ¹⁶ E. Raub and F. Sautter, *Metalloberfläche*, **11**, 249 (1957).
- ¹⁷ N.P. Fedotev and P.M. Vyacheslavov, *Plating*, **57**, 700 (1970).
- ¹⁸ K.M. Gorbunova and Yu.M. Polukarov, *Electrocrystallisation of alloys*, in *Electrodeposition of alloys*, V.A. Averkin Ed., Israel Program for Scientific Translation, Jerusalem (1964); p. 29.
- ¹⁹ L. Haiying, M. Chikazawa, and T. Watanabe, *J. Japan Inst. Metals*, **63**(4), 474 (1999).
- ²⁰ I.V. Mironow and L.D. Tselodub, *J. Solution Chem.* **25**(3), 315 (1996).
- ²¹ N. Saunders and A.P. Miodownik, *Calphad*, **9**, 159 (1987).